NANO LETTERS

2007
Vol. 7, No. 6
1692−1696

Disassembly of Nanodiscs with Cholate

Amy Y. Shih,[†,‡] Peter L. Freddolino,[†,‡] Stephen G. Sligar,[†,‡,§] and Klaus Schulten*[,†,‡,||]

Center for Biophysics and Computational Biology, Beckman Institute for Advanced Science and Technology, Departments of Physics and Biochemistry, University of Illinois at Urbana−Champaign, Urbana, Illinois 61801

Received March 23, 2007; Revised Manuscript Received April 30, 2007

ABSTRACT

Nanodiscs are protein–lipid particles that furnish a nanometer-sized membrane environment for the investigation of membrane proteins. Nanodiscs assemble spontaneously upon the removal of cholate from an initial mixture of cholate, lipids, and engineered amphipathic proteins. A combined experimental-computational approach is applied here to study the disassembly of nanodiscs through the addition of cholate to preformed particles. For this purpose, small-angle X-ray scattering experiments and coarse-grained molecular dynamics simulations were performed and compared. The study offers a detailed view of nanodisc dynamics.

Nanodiscs are nanometer-sized self-assembled discoidal particles consisting of engineered amphipathic helical proteins that wrap themselves around the circumference of a lipid bilayer in a beltlike manner,[1−5] as seen in Figure 1. Nanodiscs self-assemble from a starting mixture containing a precise ratio of proteins (called membrane scaffold proteins), lipids, and the detergent cholate. The self-assembly process is initiated by the removal of cholate and results in the formation of homogeneous discoidal particles of discrete size and composition.[1,6]

Nanodiscs[7−9] furnish a "native-like" membrane environment in which one can embed single membrane proteins with defined oligomerization states (i.e., monomers, dimers, etc.), allowing researchers to easily investigate them one by one. Nanodiscs have already been used as platforms for studying membrane proteins such as cytochrome P450s,[10−16] bacteriorhodopsin,[17,18] bacterial chemoreceptors,[19] β2 adnergenic receptors,[20] and blood clotting factors.[21] Additionally, because nanodiscs are nanometer-sized and homogeneous, they make ideal platforms for studying phase transitions of finite lipid bilayers.[22,23] Nanodiscs are also of interest for the study of the membrane scaffold proteins themselves,[24] in particular because these scaffold proteins are engineered from human apolipoprotein A-I (apo A-I), the major protein component in high-density lipoproteins (HDL). Indeed, information from nanodisc structure and assembly can provide insight into the formation of HDL particles that are highly health relevant because low levels of HDL are a risk factor for coronary heart disease and atherosclerosis.[25]

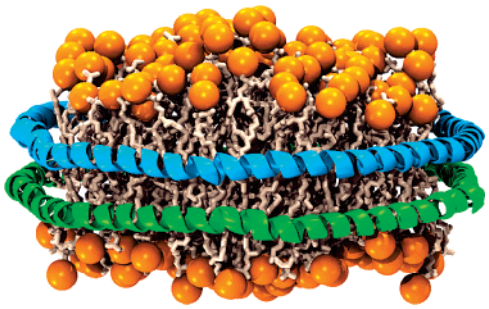

Figure 1. Schematic view of a nanodisc. Nanodiscs are nanometer-sized discoidal particles with two membrane scaffold proteins (shown in blue and green) wrapped around a lipid bilayer (shown with the lipid headgroups in orange, and the lipid tails in light tan) in a beltlike manner. The view is based on an all-atom structure; water surrounding the nanodisc is not shown.

Nanodiscs have been studied extensively,[1,2,5,6,22−24] but the assembly process and final geometry, in which two scaffold proteins surround a disclike lipid bilayer (Figure 1),[2,24,26−38] are still poorly characterized; due to the inherently disordered nature of the lipid bilayer, conventional experimental methods offer only limited structural resolution. Among these methods, small-angle X-ray scattering (SAXS) is one of the most promising,[2,6,23,39,40] in particular when complemented by computational modeling of nanodiscs.[2,4,5] Such modeling provides highly resolved structural and dynamical descriptions that can be compared to and verified by SAXS. Such a combined experimental-computational approach is applied here to study the process inverse to assembly, namely disassembly of nanodiscs through the addition of increasing concentrations of cholate to preformed nanodiscs. For this purpose, the process of nanodiscs disassembly with cholate was monitored by experimental SAXS. Coarse-grained (CG) molecular dynamics (MD) simulations were performed on

* To whom correspondence should be addressed. E-mail: kschulte@ks.uiuc.edu.
[†] Center for Biophysics and Computational Biology.
[‡] Beckman Institute for Advanced Science and Technology.
[§] Department of Biochemistry.
[||] Department of Physics.

10.1021/nl0706906 CCC: $37.00
Published on Web 05/16/2007

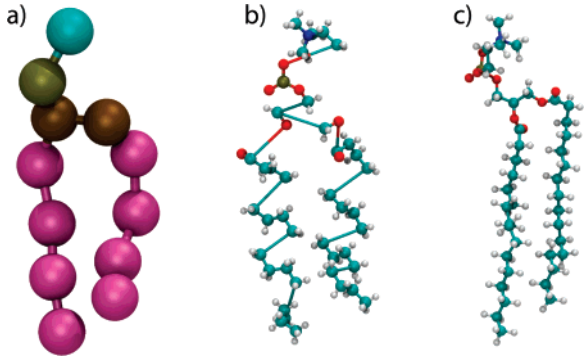

Figure 2. Reverse coarse-graining of a CG structure into an all-atom representation. The CG structure (a) is reverse coarse-grained by placing the center of mass of the group of atoms represented by a single CG bead to the location of that CG bead (b). The all-atom structure is then energy minimized and equilibrated with restraints in order to generate the final all-atom structure (c).

the same disassembly process and the results compared to the observed SAXS. Studying the disassembly of nanodiscs should also shed light on the mechanism of nanodisc self-assembly.

CG MD simulations were performed using the program NAMD 2.5[41] to generate a preformed and equilibrated nanodisc structure in which two MSP1 Δ(1−11) (also previously referred to as MSP1D1(−))[6] membrane scaffold proteins are wrapped around a central core of 160 DPPC lipids (80 per leaflet) in a beltlike fashion.[4,5] Subsequently, cholate molecules were randomly added to the simulation cell surrounding the nanodiscs in concentrations of 5, 10, 50, 100, and 320 cholates per nanodisc (see Figure S1 provided in Supporting Information). Each nanodisc system was solvated with a minimum of 15 Å of CG water and neutralized using CG sodium ions, resulting in system sizes consisting of between 12 000 CG beads for the nanodisc without cholate to 36 000 CG beads for the nanodisc with 320 cholate molecules. Typically, a ratio of 2 cholate molecules per lipid molecule is used when preparing nanodiscs and thus is chosen here as the maximal cholate concentration. Nanodisc disassembly is likely to require microseconds or longer, which is too long for traditional all-atom MD simulations. Therefore, we described the process by means of CG MD simulations that were already successfully applied to simulate nanodisc assembly.[4,5] For each cholate concentration, the CG simulations lasted long enough, i.e., between 1 and 2 μs, to observe equilibration or disassembly.

To compare the CG simulation results with experimental SAXS data, the resulting CG structures were reverse coarse-grained, as shown in Figure 2, into all-atom structures by mapping the center of mass of the group of atoms represented by a single CG bead to that beads location, using the CGTools plugin[42] in VMD 1.8.5.[43] The generated all-atom structure was energy minimized and equilibrated for 500 ps using NAMD 2.6[41] with the CHARMM27 force field for lipids[44] and the CHARMM22 force field for proteins with CMAP corrections.[45] This procedure resulted in an all-atom structure from which SAXS curves were calculated using the program CRYSOL.[46] The resulting all-atom structures can also be used for further atomistic simulations, e.g., to determine physical properties. The calculated SAXS curves were compared with experimental SAXS curves obtained for nanodiscs containing increasing concentrations of cholate. For the experiments, nanodiscs were prepared as previously described,[1] cholate was then added to the preformed particles in concentrations of 5, 10, 50, and 100 cholates per particle, and their SAXS curves measured at 46 °C at DND-CAT 5 at the Advanced Photon Source, Argonne, IL. Distance distributions for both simulated and experimental SAXS curves were calculated using the program GNOM.[47] A more detailed description of the various methods used in this study can be found in the Supporting Information.

The results of the CG simulations of nanodiscs without cholate and with various concentrations of cholate are shown in Figure 3. In the disassembly simulations, the cholate molecules were observed to insert themselves primarily along the interface of the membrane scaffold proteins and the lipid bilayer (see movie provided in Supporting Information). Indeed, the cholate molecules do not insert themselves into the hydrophobic tail regions of the lipid bilayers; rather, they adhere first to the interface of lipid head and tail groups, essentially floating on the surface of the lipid bilayer until they insert themselves between the membrane scaffold proteins and the lipids.

The addition of small numbers (5−10) of cholate into nanodiscs (Figure 3b,c) does not significantly perturb the discoidal shape, the arrangement of the scaffold proteins along the circumference of the lipid bilayer, or the overall disc diameter. Only a slight increase in the disc diameter from 10.3 to 10.4 nm was observed with the addition of up to 10 cholate molecules per nanodisc. This suggests that, for the experimental self-assembly of nanodiscs, a few leftover cholate molecules would have little or no effect on the overall particle shape or size.

SAXS measurements calculated from CG simulations of preformed nanodiscs and nanodiscs with the addition of 5 or 10 cholates per particle qualitatively match those measured experimentally (Figure 4a−c). The calculated SAXS curves exhibit a sharp minimum followed by a broad maximum, which is typical of nanodiscs[2,6,23] and which are similarly seen in the experimental measurements. The calculated distance distribution, $p(R)$, from these SAXS measurements (Figure 5) reveals that the overall diameter (10.3−10.4 nm) and bilayer thickness (∼5.2 nm) of simulated and experimental systems are comparable.

Adding larger amounts of cholate results in structural changes of the nanodiscs. The addition of 50 or 100 cholates produces an opening of the scaffold proteins that encircle the lipid bilayer as revealed by an increase in particle diameter from 10.3 to 10.9 nm and 12.0 nm, respectively (Figure 3d,e; movie in Supporting Information). The ability of the scaffold protein to open and incorporate additional molecules can explain the size heterogeneity seen in native discoidal HDL particles.[48,49]

The incorporation of a large amount of cholate molecules into nanodiscs causes the scaffold proteins to fluctuate at the circular edge of the lipid bilayer, however, without slipping off the edge and coming to lie on top of the lipid

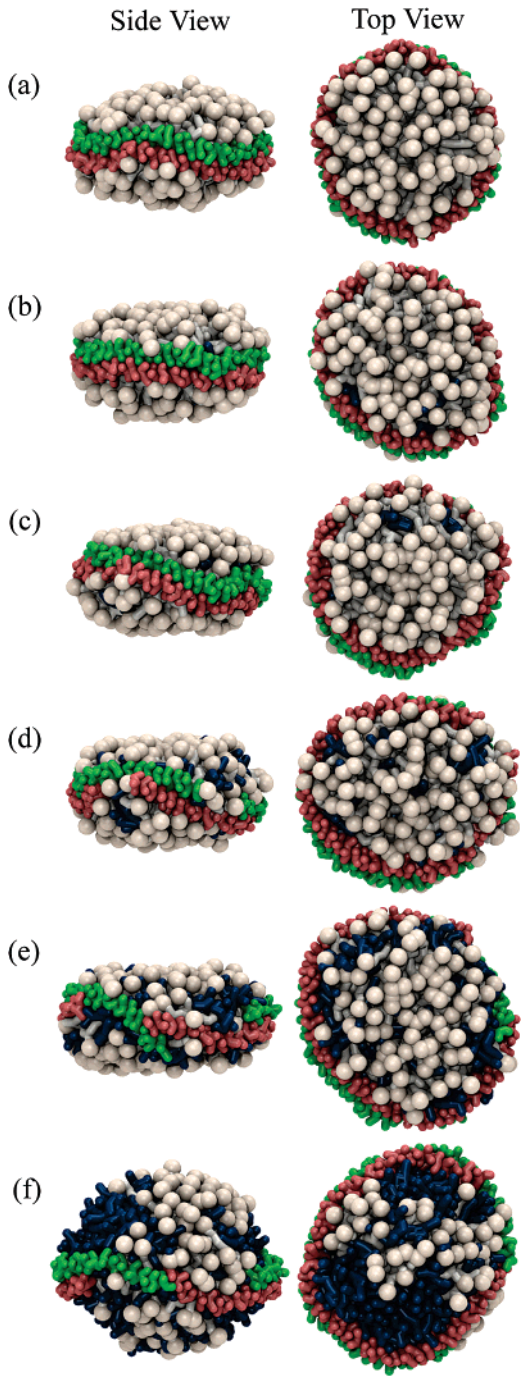

Figure 3. CG MD simulations of a nanodisc absorbing increasing concentrations of cholate. Shown is an equilibrated nanodisc without cholates (a) in which two membrane scaffold proteins (in red and green) encircle a 160 DPPC lipid bilayer (in tan). To this nanodisc, 5 (b), 10 (c), 50 (d), 100 (e), and 320 (f) cholate molecules (shown in blue) were added. The resulting systems were simulated until a stationary state was reached at 1−2 μs. Shown are the final states for each nanodisc−cholate aggregate; water is not shown. The nanodisc−cholate dynamics are shown in an illustrative movie for case (e) (see Supporting Information).

bilayer. The cholate molecules eventually move into the interface between membrane scaffold proteins and the lipid bilayer (Figure 3; movie in Supporting Information). This behavior is likely due to the hydroxyl groups in the steroidal body of cholate, which renders cholate less hydrophobic than the DPPC lipid tails.

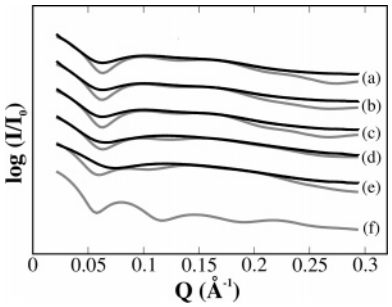

Figure 4. SAXS curves from experimental measurements (in black) and calculated for simulated structures (in gray) of nanodiscs containing 0, 5, 10, 50, 100, and 320 cholate molecules (a−f, respectively). For nanodiscs containing 320 cholate molecules, an experimental SAXS curve was not obtained as such a system disassembles into a disperse protein−lipid−cholate mixture.

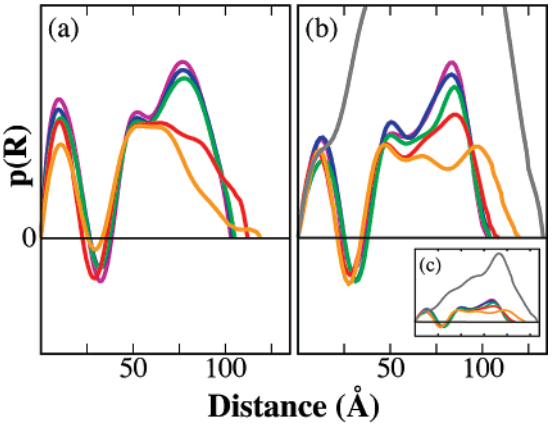

Figure 5. Distance distributions. The detailed distributions, $p(R)$, shown are calculated for experimental (a) and simulated structures (b) of nanodiscs containing from 0 (purple), 5 (blue), 10 (green), 50 (red), 100 (orange), to 320 (gray) cholates per disc. (c) The distance distributions are scaled down to show all the curves. Note that the plotted densities are relative to that of bulk water.

For nanodiscs with 50 or 100 cholate molecules per particle, computed and observed SAXS curves (Figure 4c,d) are not as well correlated as they are in the case of nanodiscs with smaller concentrations of cholate. A comparison of the simulated and observed SAXS curves shows that larger amounts of cholate results, for the experimental SAXS curves, in a shift of the sharp minimum to larger scattering vectors (Q), whereas the simulated SAXS curves show a shift of the minimum to smaller scattering vectors as well as the development of a slight second minimum. The distance distribution calculated from the SAXS data indicates that, although the experimental and simulated nanodiscs with 50 or 100 cholate molecules are comparable in overall diameter, the experimental nanodiscs appear to be less stable than the simulated ones, particularly in regard to the scaffold proteins (Figure 5). This is evident as judged by the loss of the peak at ∼79 Å, which suggests the scaffold proteins are no longer arranged around the circumference of the lipid bilayer, having instead "slipped off the edge" and onto the surface of the bilayer, as seen in the increase in the peak between 50 and 70 Å (Figure 5a). The arrangement of the scaffold proteins on the surface of the lipid bilayer was observed in previous CG simulations of nanodisc assembly.[5] The discrepancy

between observation and computation could be due to a number of factors including insufficient sampling in the simulations or errors in the CG force field. We note that significantly improved sampling through longer simulations is technically unfeasible at present.

CG simulations were also performed on a nanodisc with 320 cholate molecules added. In this case, the nanodisc assumed a spherical liposomal structure (Figure 3f), 13.3 nm in diameter. The lipid and cholate formed a liposome structure with a water core on the inside and scaffold protein on the outside. Upon reverse coarse-graining and subsequent all-atom MD simulations of nanodiscs with 320 cholates, the liposomal structure was seen to have numerous water pockets throughout the lipid−cholate mixture (see Figure S2 in Supporting Information), which is a telling sign of later disassembly into heterogeneous particles. Such a complete disassembly of the nanodisc particle is expected with the addition of 320 cholate molecules, as these are the typical starting ratios used when experimentally assembling nanodiscs.[1,6]

The close correlation between experimental and simulated SAXS measurements for nanodiscs containing small quantities of cholate provides insight into the behavior of nanodiscs absorbing larger quantities of cholate, even though no such close correlation can be found for the latter case. The simulations clearly suggest that cholate does not insert itself into the hydrophobic lipid bilayer, preferring instead to interact at the lipid head and tail interface as well as at the interface between lipid bilayer and membrane scaffold protein.

From the present disassembly simulations and previous assembly simulations (in the absence of cholate)[5] emerges a mechanism of nanodisc assembly that starts from an initial mixture with a stoichiometry of 320 cholates, 160 DPPC lipids, and two scaffold proteins. The removal of cholate initiates the self-assembly process by allowing the lipids and scaffold proteins to aggregate, forming large spherical particles. These spherical particles likely have a core consisting of lipids and cholate, with the scaffold proteins oriented in a random fashion along the surface. Once enough cholate has been removed, the lipids form a bilayer resulting in the transformation from spherical to discoidal particles (the difference between the two corresponding to the difference between the spherical 320 cholates per nanodisc and 100 cholates per nanodisc particles shown in Figure 4e,f). Upon removal of the majority of cholate, nanodiscs form in which a discoidal lipid bilayer is encircled by the membrane scaffold proteins. The membrane scaffold proteins continue to rearrange themselves until finally reaching the equilibrium double-belt configuration.

In conclusion, we have combined experimental and computational studies of nanodisc disassembly through addition of cholate to preformed nanodiscs. CG MD simulations provided high-resolution images of the disassembly process that were compared with and tested through low-resolution SAXS measurements. The results offer an unprecedented detailed view of nanodisc disassembly. Cholate molecules were found to preferentially insert themselves into the nanodiscs at the interface between lipid bilayer and scaffold protein. The presence of small amounts of cholate (5−10 molecules) in nanodiscs does not significantly alter the overall size or shape of the particle, nor does it affect the scaffold proteins. However, larger amounts of cholate were found to alter the overall structure of nanodiscs increasing the overall particle diameter, and at very high concentrations, leading to spherical particles in which cholate and lipids form a liposome encircled by membrane scaffold proteins.

Acknowledgment. We thank Drs. Timothy Bayburt and Ilia Densiov for advice on preparing nanodiscs and analysis of SAXS data, and Steven Weigand and Dr. Denis Keane for their expertise in setting up the beamline. This work is supported by grants RO1-GM067887, P41-RR05969, and RO1-GM33775 from the National Institutes of Health to K.S. and S.G.S. We acknowledge supercomputer time provided by the National Science Foundation grant MCA93S028. Portions of this work were performed at the DuPont−Northwestern−Dow Collaborative Access Team (DND-CAT) Synchrotron Research Center located at Sector 5 of the Advanced Photon Source. DND-CAT is supported by the E. I. DuPont de Nemours and Co., the Dow Chemical Company, the U.S. National Science Foundation through grant DMR-9304725, and the State of Illinois through the Department of Commerce and the Board of Higher Education grant IBHE HECA NWU 96. Use of the Advanced Photon Source was supported by the U.S. Department of Energy, Office of Science, Office of Basic Energy Sciences, under contract no. W-31-109-Eng-38.

Supporting Information Available: Detailed description of the methods, movies (MPG) of the insertion of cholate into nanodiscs, migration of cholate to the circumference of the nanodiscs, and opening up of the membrane scaffold proteins (including fluctuations of scaffold proteins along the edge of the nanodisc), and a figure depicting the formation of water channels in nanodiscs with 320 cholates. This material is available free of charge via the Internet at http://pubs.acs.org.

References

(1) Bayburt, T. H.; Grinkova, Y. V.; Sligar, S. G. *Nano Lett.* **2002**, *2*, 853−856.
(2) Shih, A. Y.; Denisov, I. G.; Phillips, J. C.; Sligar, S. G.; Schulten, K. *Biophys. J.* **2005**, *88*, 548−556.
(3) Lu, D.; Aksimentiev, A.; Shih, A. Y.; Cruz-Chu, E.; Freddolino, P. L.; Arkhipov, A.; Schulten, K. *Phys. Biol.* **2006**, *3*, S40−S53.
(4) Shih, A. Y.; Arkhipov, A.; Freddolino, P. L.; Schulten, K. *J. Phys. Chem. B* **2006**, *110*, 3674−3684.
(5) Shih, A. Y.; Freddolino, P. L.; Arkhipov, A.; Schulten, K. *J. Struct. Biol.* **2007**, *157*, 579−592.
(6) Denisov, I.; Grinkova, Y.; Lazarides, A.; Sligar, S. *J. Am. Chem. Soc.* **2004**, *126*, 3477−3487.
(7) Sligar, S. G. *Biochem. Biophys. Res. Commun.* **2003**, *312*, 115−119.
(8) Service, R. F. *Science* **2004**, *304*, 674.
(9) Nath, A.; Atkins, W. M.; Sligar, S. G. *Biochemistry* **2007**, *46*, 2059−2069.
(10) Bayburt, T. H.; Sligar, S. G. *Proc. Natl. Acad. Sci. U.S.A.* **2002**, *99*, 6725−6730.
(11) Civjan, N. R.; Bayburt, T. H.; Schuler, M. A.; Sligar, S. G. *Biotechniques* **2003**, *35*, 556−560, 562−563.

(12) Baas, B. J.; Denisov, I. G.; Sligar, S. G. *Arch. Biochem. Biophys.* **2004**, *430*, 218−228.
(13) Duan, H.; Civjan, N. R.; Sligar, S. G.; Schuler, M. A. *Arch. Biochem. Biophys.* **2004**, *424*, 141−153.
(14) Davydov, D. R.; Fernando, H.; Baas, B. J.; Sligar, S. G.; Halpert, J. R. *Biochemistry* **2005**, *44*, 13902−13913.
(15) Denisov, I. G.; Grinkova, Y. V.; Baas, B. J.; Sligar, S. G. *J. Biol. Chem.* **2006**, *281*, 23313−23318.
(16) Denisov, I. G.; Baas, B. J.; Grinkova, Y. V.; Sligar, S. G. *J. Biol. Chem.* **2007**, *282*, 7066−7076.
(17) Bayburt, T. H.; Sligar, S. G. *Protein Sci.* **2003**, *12*, 2476−2481.
(18) Bayburt, T. H.; Grinkova, Y. V.; Sligar, S. G. *Arch. Biochem. Biophys.* **2006**, *450*, 215−222.
(19) Boldog, T.; Grimme, S.; Li, M.; Sligar, S. G.; Hazelbauer, G. L. *Proc. Natl. Acad. Sci. U.S.A.* **2006**, *103*, 11509−11514.
(20) Leitz, A.; Bayburt, T.; Barnakov, A.; Springer, B.; Sligar, S. *Biotechniques* **2006**, *40*, 601−612.
(21) Shaw, A. W.; Pureza, V. S.; Sligar, S. G.; Morrissey, J. H. *J. Biol. Chem.* **2007**, *282*, 6556−6563.
(22) Shaw, A. W.; McLean, M. A.; Sligar, S. G. *FEBS Lett.* **2004**, *556*, 260−264.
(23) Denisov, I.; McLean, M.; Shaw, A.; Grinkova, Y.; Sligar, S. *J. Phys. Chem. B* **2005**, *109*, 15580−15588.
(24) Li, Y.; Kijac, A. Z.; Sligar, S.; Rienstra, C. M. *Biophys. J.* **2006**, *91*, 3819−3828.
(25) Wang, X.; Olsen, L.; Roderick, S. *Structure* **2002**, *10*, 581−588.
(26) Segrest, J. P.; Jones, M. K.; Klon, A. E.; Sheldahl, C. J.; Hellinger, M.; De Loof, H.; Harvey, S. C. *J. Biol. Chem.* **1999**, *274*, 31755−31758.
(27) Koppaka, V.; Silvestro, L.; Engler, J.; Brouillette, C.; Axelsen, P. *J. Biol. Chem.* **1999**, *274*, 14541−14544.
(28) Segrest, J. P.; Harvey, S. C.; Zannis, V. *Trends Cardiovasc. Med.* **2000**, *10*, 246−252.
(29) Li, H.; Lyles, D. S.; Thomas, M. J.; Pan, W.; Sorci-Thomas, M. G. *J. Biol. Chem.* **2000**, *275*, 37048−37054.
(30) Panagotopulos, S.; Horace, E.; Maiorano, J.; Davidson, W. *J. Biol. Chem.* **2001**, *276*, 42965−42970.
(31) Tricerri, M. A.; Behling, Agree, A. K.; Sanchez, S. A.; Bronski, J.; Jonas, A. *Biochemistry* **2001**, *40*, 5065−5074.
(32) Klon, A. E.; Segrest, J. P.; Harvey, S. C. *Biochemistry* **2002**, *41*, 10895−10905.
(33) Klon, A. E.; Segrest, J. P.; Harvey, S. C. *J. Mol. Biol.* **2002**, *324*, 703−721.
(34) Li, L.; Chen, J.; Mishra, V. K.; Kurtz, J. A.; Cao, D.; Klon, A. E.; Harvey, S. C.; Anantharamaiah, G.; Segrest, J. P. *J. Mol. Biol.* **2004**, *343*, 1293−1311.
(35) Silva, R. A. G. D.; Hilliard, G. M.; Li, L.; Segrest, J. P.; Davidson, W. S. *Biochemistry* **2005**, *44*, 8600−8607.
(36) Davidson, W. S.; Gangani, R. A.; Silva, D. *Curr. Opin. Lipidol.* **2005**, *16*, 295−300.
(37) Gorshkova, I. N.; Liu, T.; Kan, H. Y.; Chroni, A.; Zannis, V. I.; Atkinson, D. *Biochemistry* **2006**, *45*, 1242−1254.
(38) Catte, A.; Patterson, J. C.; Jones, M. K.; Jerome, W. G.; Bashtovyy, D.; Su, Z.; Gu, F.; Chen, J.; Aliste, M. P.; Harvey, S. C.; Li, L.; Weinstein, G.; Segrest, J. P. *Biophys. J.* **2006**, *90*, 4345−4360.
(39) Sachs, J. N.; Petrache, H. I.; Woolf, T. B. *Chem. Phys. Lipids* **2003**, *126*, 211−223.
(40) Zagrovic, B.; Jayachandran, G.; Millett, I. S.; Doniach, S.; Pande, V. S. *J. Mol. Biol.* **2005**, *353*, 232−41.
(41) Phillips, J. C.; Braun, R.; Wang, W.; Gumbart, J.; Tajkhorshid, E.; Villa, E.; Chipot, C.; Skeel, R. D.; Kale, L.; Schulten, K. *J. Comput. Chem.* **2005**, *26*, 1781−1802.
(42) CGTools Plugin in VMD, http://www.ks.uiuc.edu/Research/vmd/plugins/cgtools/.
(43) Humphrey, W.; Dalke, A.; Schulten, K. *J. Mol. Graphics* **1996**, *14*, 33−38.
(44) MacKerell, A. D., Jr.; Bashford, D.; Bellott, R. L.; Dunbrack, R. L., Jr.; Evanseck, J. D.; Field, . J.; Fischer, S.; Gao, J.; Guo, H.; Ha, S.; Joseph-McCarthy, D.; Kuchnir, L.; Kuczera, K.; Lau, F. T. K.; Mattos, C.; Michnick, S.; Ngo, T.; Nguyen, D. T.; Prodhom, B.; Reiher, W. E., III; Roux B.; Schlenkrich, M.; Smith, J. C.; Stote, R.; Straub, J.; Watanabe, M.; Wiorkiewicz-Kuczera, J.; Yin, D.; Karplus, M. *J. Phys. Chem. B* **1998**, *102*, 3586−3616.
(45) MacKerrel, A. D., Jr.; Feig, M.; Brooks, C. L., III. *J. Comput. Chem.* **2004**, *25*, 1400−1415.
(46) Svergun, D. I.; Barberato, C.; Koch, M. H. J. *J. Appl. Crystallogr.* **1995**, *28*, 768−773.
(47) Svergun, D. I. *J. Appl. Crystallogr.* **1992**, *25*, 495−403.
(48) Jonas, A. *Methods Enzymol.* **1986**, *128*, 553−582.
(49) Jonas, A.; Kézdy, K. E.; Wald, J. H. *J. Biol. Chem.* **1989**, *264*, 4818−4824.

NL0706906